

Fano-type interference in the Raman spectrum of photoexcited Si

Valentin Magidson* and Robert Beserman

Technion - Israel Institute of Technology, Haifa, Israel

(Received 16 March 2002; published 11 November 2002)

Free carriers introduced by high cw laser power densities (2×10^6 to 4×10^7 W/cm²) in silicon result in a Fano-type asymmetric Raman line shape. This line shape is attributed to the interaction between the photoexcited holes and the zone center optical phonon. Raman spectra of photoexcited Si are compared with *p*-doped Si spectra in a wide temperature range (5–750 K) for different laser wavelengths. The determination of the free carrier plasma concentration from the Raman spectrum is demonstrated. These measurements provide an additional source of information on recombination rates, ambipolar diffusion, and electron-phonon coupling parameters for dense electron-hole plasma (up to 4×10^{19} cm⁻³).

DOI: 10.1103/PhysRevB.66.195206

PACS number(s): 78.30.Am, 61.80.Ba, 63.20.Kr

I. INTRODUCTION

Electron-hole plasma properties in Si are important in both basic many-body physics and wide range of applications. In this paper, we present a Raman spectroscopy study of the electron-hole plasma in Si excited by cw lasers. To the best of our knowledge, the Fano-type interference in Si with the electron-hole plasma has not been systematically studied. This interference has been observed only in experiments with high-power pulsed laser excitation,¹ along with the sample heating to submelting temperatures. In this case the Fano interference gives only a small contribution on the background of large thermal line broadening, and both effects cannot be separated unambiguously. In these experiments the laser spot diameter was large compared to the laser penetration depth, so that in the center of the laser spot one-dimensional heat transfer takes place, resulting in very high temperatures for the excitation density used.

In this work we make use of efficient three-dimensional heat dissipation when the laser beam is focused to the sub-micron size spot, to reduce the sample heating for given excitation density. Free carrier plasma concentration of 3×10^{19} cm⁻³ has been achieved with the sample heating of only 100 °C. The free carrier plasma concentration was estimated by comparison with the Raman spectra of some heavily doped samples in a wide temperature range, used as a calibration.

In contrast to the large amount of experimental data² for free carrier concentrations below 10^{18} cm⁻³, for higher concentrations measurements of temperature dependence of such parameters as ambipolar diffusivity and Auger coefficient are quite sparse.^{3–5} In experiments involving pulsed laser excitation, such as time resolved photoluminescence and transient grating, the material parameter extraction is not straightforward for this concentration range, because many nonlinear parameters are involved simultaneously (lifetime reduction, band-gap narrowing, carrier-carrier scattering, etc.).

The Fano-type interference in Raman scattering has been extensively studied in heavily doped silicon.^{6,7} It is known to result in asymmetric line shape of the first order phonon Raman peak for both *n*-type^{8,9} and *p*-type^{10,11} silicon, when the overlapping of energies between the continuous spectrum

of Raman allowed free-carrier transitions and the quasidiscrete phonon spectrum takes place. For *p*-type Si this overlapping takes place for almost any value of the carrier concentration,¹⁰ while for *n*-type Si it takes place only above certain concentration,⁸ which is estimated¹² to be about 4×10^{19} cm⁻³. The interference results in the Fano line shape,¹³

$$I(\omega) = C + \sigma_0(q + \varepsilon)^2 / (q + \varepsilon^2), \quad \varepsilon = (\omega - \omega_0) / \Gamma, \quad (1)$$

where ω is the scattered photon energy, Γ and ω_0 are resonance width and energy, respectively, σ_0 and C are constants, and q is the symmetry parameter. In the limit of $q \rightarrow \infty$ this line shape becomes a symmetric Lorentzian. We will define $1/q$ as an asymmetry parameter. It is roughly proportional to the free carrier concentration, as reported in the literature.^{10,11}

II. EXPERIMENT

Floating zone lightly doped 3×10^{15} cm⁻³ Si(100) wafer was used as “pure” silicon sample. This doping concentration is negligible for the Fano interference process. A thermal oxide layer of 75 nm thickness provides both passivation of surface recombination centers and antireflection coating, reducing the reflectivity to 10%–15% for the laser wavelengths used. Si wafers heavily doped by boron (*p*-type) and arsenic (*n*-type) were used as reference samples.

The Dilor micro-Raman system was used to investigate the Raman scattering in the backscattering configuration. A microscope objective with numerical aperture (NA) 0.95 was used at room temperatures, and with NA 0.55 at low temperatures, resulting in a spot size (e^{-1} full width) of approximately 0.6λ and λ , respectively¹⁴ (λ is the laser wavelength). For the low temperature measurements the sample was attached with indium to the cold finger of a He cryostat for efficient heat sinking. For high temperature measurements a Linkam oven was used. An Ar⁺ laser with 514.5 nm wavelength and three Dye lasers tuned to 600 nm, 650 nm, and 708 nm wavelength operated in the cw mode were used for excitation. The penetration depth for these lasers is 1 μ m, 2 μ m, 3 μ m, and 5 μ m, respectively.

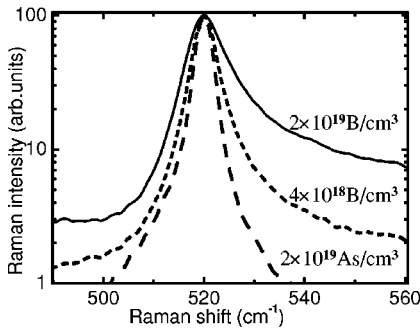


FIG. 1. Raman spectra at 300 K of *p*-type doped Si with 4×10^{18} B/cm³ (short dashed line), 2×10^{19} B/cm³ (solid line), and *n*-type Si doped with 2×10^{19} As/cm³ (long dashed line).

III. RESULTS

A. High temperature measurements

Figure 1 presents the Raman spectra of doped Si at 300 K. For *p*-type samples 4×10^{18} B/cm³ and 2×10^{19} B/cm³ there is a Fano-type asymmetric broadening to the high energies. For *n*-type sample with 2×10^{19} As/cm³ no asymmetry is observed, because this concentration is lower than the Fano interference threshold for *n*-type Si (Refs. 8,12) (about 4×10^{19} cm⁻³). As seen later, in our experiments the concentration of photo-excited plasma is estimated to be below 4×10^{19} cm⁻³, so that the influence of electrons to the Fano interference process may be neglected. Above this Fano threshold the asymmetry of Raman peak for *n*-type Si is smaller, and opposite in sign, to that of *p*-type Si with the same concentration. For the photoexcited free carrier plasma with equal concentration of electrons and holes, the contribution of electrons to the Fano interference may be neglected to a first approximation.¹

Broadening of the first-order Raman line to the high energy is a “fingerprint” of the hole Fano-type interference. Other possible factors which are known to influence the shape of the Raman line, such as, heating, impurities, lattice imperfections, etc., generally cause the line to broaden towards the low energy side of the peak.

Figure 2 shows the dependence of Fano asymmetry pa-

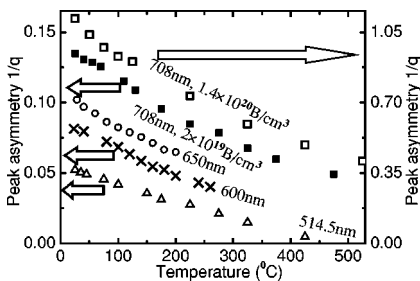


FIG. 2. Fano asymmetry parameter $1/q$ of *p*-type doped samples as a function of the oven temperature, measured with different laser wavelength: 708 nm (squares), 650 nm (circles), 600 nm (crosses), and 514.5 nm (triangles). The upper line (open squares) represents the 1.4×10^{20} B/cm³ sample spectra asymmetry (right axis). Other four lines represents the 2×10^{19} B/cm³ sample spectra asymmetry (left axis). The right to left axes ratio is 7.

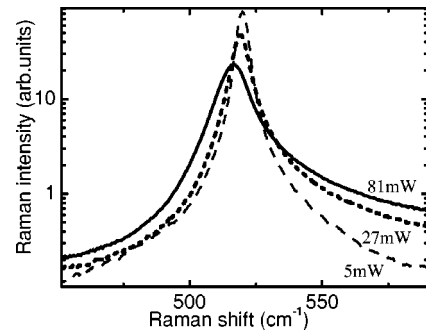


FIG. 3. Raman spectra of Si excited by the diffraction limited focused laser beam (514.5 nm): 5 mW (long dashed line), 27 mW (short dashed line), and 81 mW (solid line). All spectra are normalized to the laser power.

rameter $1/q$ on the temperature of the oven heated sample for different laser wavelengths. Four lines represent the asymmetry of the 2×10^{19} B/cm³ sample (left axis), which is decreasing with increasing temperature and increasing with probing photon wavelength. The upper line (open squares) corresponds to the 1.4×10^{20} B/cm³ sample measured with a 708 nm laser, and the asymmetry values are indicated on the right axis. The scale on the right-hand side of Fig. 2 is equal to the scale on the left-hand side multiplied by 7, which is the doping concentration ratio with the 2×10^{19} B/cm³ (sample). One can see that this line (open squares) is close to values for the 2×10^{19} B/cm³ sample measured with the same laser wavelength (full squares). It confirms our assumption that the $1/q$ parameter is approximately proportional to the concentration of holes for all relevant temperatures.

Stokes and anti-Stokes spectra were measured for lightly doped Si at different laser excitation densities. All spectra were fitted with the Fano formula [Eq. (1)]. The fit residuals are smaller than 3% of the peak height in the ± 40 cm⁻¹ spectral range. Figure 3 presents a few Stokes spectra measured with the 514.5 nm laser normalized to the laser power. Fano-type asymmetry increases with laser power. Figure 4 presents a few residuals of Fano fit to high laser power spectra, which are attributed to the heating of the Si-SiO₂ interface. When this residual peak is approaching 505 cm⁻¹ (which corresponds to 700–800 °C), the upper SiO₂ layer melts and the Si surface is destroyed by oxidation. It has

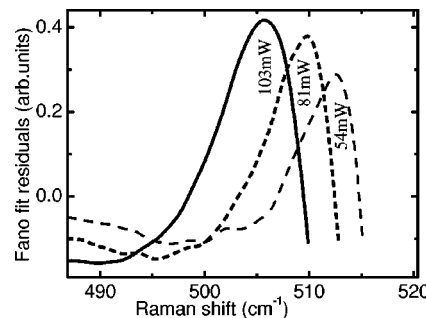


FIG. 4. Residuals of the Fano fit to the Raman spectra of Si excited high power laser beam (514.5 nm): 54 mW (long dashed line), 81 mW (short dashed line), and 103 mW (solid line).

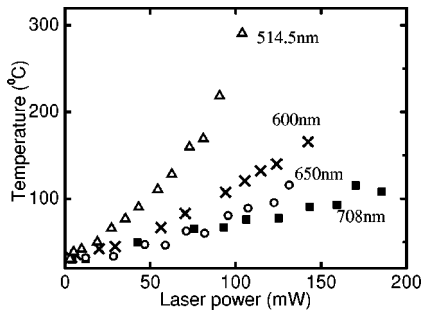


FIG. 5. Temperature calculated from the Stokes to anti-Stokes ratio of the Raman spectra of Si excited with different laser wavelengths: 708 nm (squares), 650 nm (circles), 600 nm (crosses), and 514.5 nm (triangles).

been checked that no Si melting takes place [the melting point of Si is 1413 °C (Ref. 2)]. The oxide melting has been obtained with 514.5 and 600 nm lasers (smaller penetration depth), while for 650 and 708 nm excitation the residual peak is not resolved due to the low laser powers available.

There are two ways to calculate an average temperature from the Raman spectra: Fig. 5 presents the temperature from the Stokes to anti-Stokes ratio,¹ and Fig. 6 presents the temperature from the spectral peak position¹⁵ (the left axis represent the peak position, and the right axis represents the corresponding temperature). The temperature is averaged on the volume that is approximately defined by the laser spot size (about 0.5 μm) and half of the laser penetration depth (from 0.5 μm to 2.5 μm depending on the laser used). One can see that for high laser powers the temperature estimated from peak positions is about 50 °C (corresponds to approximately -1 cm^{-1}) higher than estimated from Stokes to anti-Stokes ratios. This may be attributed to an additional spectral shift due to the phonon-hole interaction, in quantitative agreement with the experiment.¹⁰

Figure 7 presents the asymmetry parameter $1/q$ as a function of the laser power for different laser wavelength. For high laser powers the slope is decreasing. The change in the slope is attributed to two factors: the first one is the nonlinear dependence of the carrier concentration on the laser power due to the nonlinear diffusion and nonlinear recombination,

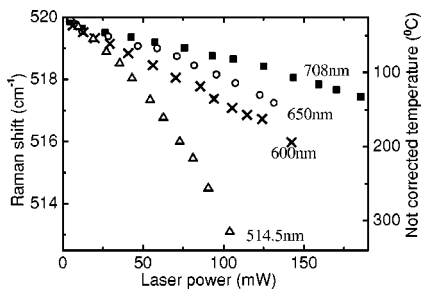


FIG. 6. Spectral position of the Raman spectra (from Fano fit) of Si excited with different laser wavelengths: 708 nm (squares), 650 nm (circles), 600 nm (crosses), and 514.5 nm (triangles). The right scale represents the temperature calculated with linear coefficient for the thermal shift (42 °C/cm^{-1}), not taking into account the Fano spectral shift.

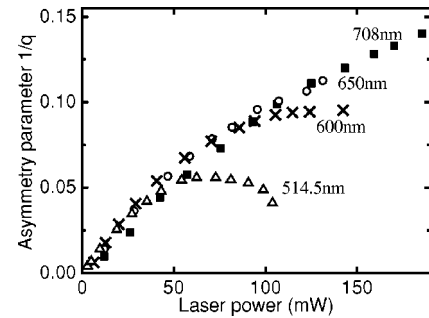


FIG. 7. Fano asymmetry parameter of the Raman spectra, measured as a function of the laser power for different excitation laser wavelengths: 708 nm (squares), 650 nm (circles), 600 nm (crosses), and 514.5 nm (triangles).

and the second one is the dependence of the $1/q$ parameter on temperature for each hole concentration.

The key point in our method is to correct the second factor by measuring the $1/q$ parameter of doped samples at different temperatures (Fig. 2). For an exact determination of the photoinduced carrier plasma concentration one has to find a p -doped sample which has the same value of the $1/q$ parameter as the photoexcited sample, when the doped sample is oven heated to the temperature of the photoexcited sample heated by the laser. One has to plot together two graphs: the graph of asymmetry versus laser power and the graph of asymmetry parameter for the doped sample oven heated to the temperature calculated from Stokes to anti-Stokes ratio. The crossing of two lines gives the laser power that excites the electron-hole plasma to the same density, as the free carrier density of the p -type doped sample. As an example, we consider 708 nm laser excitation and $2 \times 10^{19} \text{ B/cm}^3$ doped sample. From Figs. 5, 2, and 4 one can see that for the laser power of 130 mW the estimated temperature is 75 °C, and for the doped sample at this temperature the peak asymmetry $1/q$ is the same as for the photoexcited sample. Figure 8 presents corresponding Stokes and anti-Stokes normalized Raman spectra. The identity of the spectral shapes confirms our basic assumption that in both cases the physical processes influencing the Raman line shape are the same: Fano interference with the zone-center optical phonon and free holes.

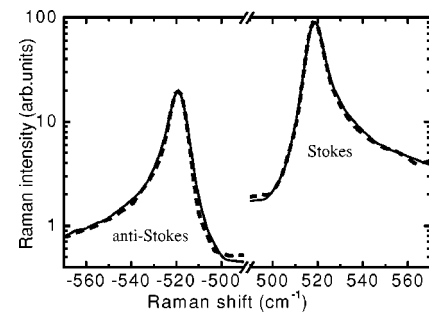


FIG. 8. Raman spectra of laser excited Si (solid line) and oven heated p -type $2 \times 10^{19} \text{ B/cm}^3$ boron doped silicon (dashed line), measured in the condition of the equal hole concentrations (see text).

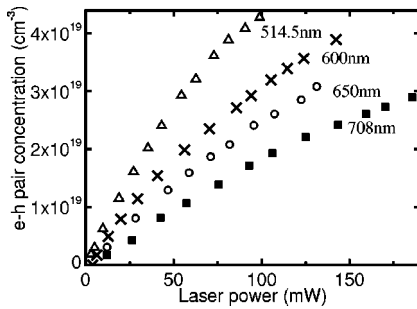


FIG. 9. Free carrier plasma concentration calculated from the asymmetry parameter $1/q$ for different laser wavelength: 708 nm (squares), 650 nm (circles), 600 nm (crosses), and 514.5 nm (triangles).

For an exact determination of photo-induced free carrier plasma one has to measure many p -type Si samples with different doping. Each reference sample gives one exact point on the graph of the plasma concentration versus laser power. For heavily doped semiconductors the dopant atoms are fully ionized, so that free carrier concentration is equal to the doping impurities concentration.¹⁶ Below the Mott transition concentration,¹⁷ one has to correct for the nonionized doping atoms to calculate the concentration of free holes in the doped sample for the given temperature.

For an approximate calculation one may use an assumption that the $1/q$ parameter is proportional to the carrier concentration. Figure 9 presents the plasma concentration calculated this way: the $1/q$ parameter is divided by the $1/q$ parameter of the doped sample at corresponding temperature and multiplied by the doping concentration ($2 \times 10^{19} \text{ cm}^{-3}$ in this case). These results are in qualitative agreement with the theoretical expectation: lasers with smaller penetration depth produce higher excitation per unit volume, and excite denser plasma for a given laser power. At large concentration the Auger recombination and nonlinear diffusion cause the nonlinear dependence on the laser power.

An infrared spectral image of the sample was measured with $1 \mu\text{m}$ spatial resolution to verify the validity of determination of the sample temperature. Photoluminescence spectra from different points of the sample have been compared to spectra from samples heated in an oven with low power laser excitation. These measurements generally confirm the temperatures obtained from Stokes to anti-Stokes ratios, but large photoluminescence width at elevated temperatures decrease the precision of this method of temperature determination.

B. Low temperature measurements

The method of determination of the electron-hole plasma concentration from Raman spectra may be extended to low temperatures. However, the algorithm used to determine concentration described above may not be used, because the anti-Stokes Raman peak is not measurable at very low temperatures, when the thermal optical phonon population is very small. In this case, the temperature determination by the Stokes to anti-Stokes ratio has to be replaced by luminescence measurements or numerical simulation. The thermal

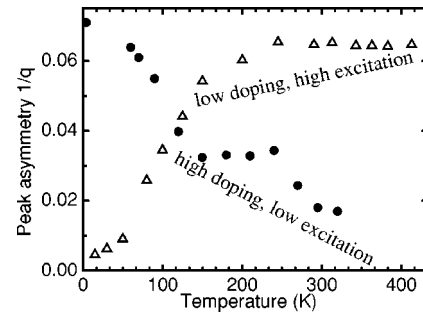


FIG. 10. Low excitation values of the $1/q$ parameter of the $4 \times 10^{18} \text{ B/cm}^3$ sample (circles), and high excitation (120 mW) values of the $1/q$ parameter for lightly doped Si. Laser wavelength is 708 nm.

conductivity of Si is very large at low temperatures,² so that to a first approximation heating may be neglected for medium excitation powers. The validity of this assumption has been checked by means of photoluminescence imaging.

Circles in Fig. 10 presents the $1/q$ parameter of the $4 \times 10^{18} \text{ B/cm}^3$ sample measured in the cryostat with low laser excitation power. One can see that the peak asymmetry decreases with increasing temperature. The flat region between 150 K and 250 K may be attributed to the reduction of the concentration of free holes at low temperatures. This flat region is not observed for samples with higher doping concentrations ($2 \times 10^{19} \text{ B/cm}^3$ and $1.4 \times 10^{20} \text{ B/cm}^3$) which have zero impurity ionization energy.¹⁶

The peak asymmetry of lightly doped Si excited with a given laser power (120 mW) shows an opposite temperature behavior, which is presented by the triangles in Fig. 10. The $1/q$ parameter is close to zero at 10 K. The peak becomes asymmetrical with increasing temperature and the $1/q$ parameter stabilizes above 300 K. This means that the concentration of the $e-h$ plasma excited under the same conditions is lower at reduced temperatures. This can be attributed to the increase of the free carrier mobility at low temperatures,² resulting in a very efficient carrier diffusion from the excitation point.

One can see that the point of interception of the two lines in Fig. 10 shows that the photoexcited plasma concentration at 110 K is the same as the hole concentration in the $4 \times 10^{18} \text{ B/cm}^3$ sample (neglecting the laser heating of the photoexcited sample).

Our explanation of the enhanced diffusion origin of the absence of observable peak asymmetry at very low temperatures is confirmed by measurements of photoexcited boron doped samples presented in Fig. 11. The hole concentration in this experiment is a sum of the concentration originating from the doping and the photoexcited plasma density. Charged boron impurities reduce the free carrier mobility, and at low temperatures become the dominant scattering centers. This results in a weaker thermal dependence of the plasma diffusivity, compared to that of intrinsic silicon. Both $2 \times 10^{19} \text{ B/cm}^3$ (squares) and $4 \times 10^{18} \text{ B/cm}^3$ (circles) samples measured with an NA0.55 objective in a He cryostat exhibit a significant increase of the peak asymmetry at the high excitation conditions (120 mW of 708 nm laser) at all temperatures.

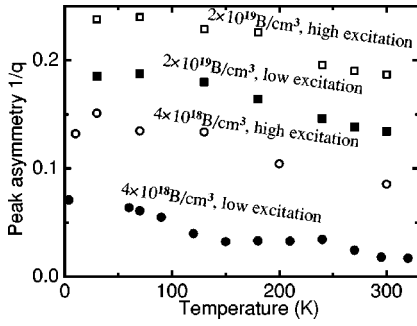


FIG. 11. Low temperature asymmetry parameter $1/q$ of 2×10^{19} B/cm³ (squares) and 4×10^{18} B/cm³ (circles) samples measured with the 708 nm laser. Full markers represent the low excitation values; open markers represent high excitation values (120 mW).

To summarize, at the low temperatures the Fano line shape analysis of Raman spectra is less suitable for the e - h density determination, because the temperature may not be deduced directly from the Raman measurements. However, it provides an optical probe of low temperature free carrier diffusivity.

IV. DISCUSSION

Numerical simulation of the Si wafer illuminated by the focused laser spot was performed using the Finite Element Method.

At the first step the equation for the free carriers distribution,

$$-\nabla(D_a \nabla(n)) + An + Bn^2 + C_a n^3 = G \quad (2)$$

is solved at the room temperature. Here n is free carrier concentration, D_a is the concentration dependent ambipolar diffusivity coefficient,⁵ A is the low injection recombination rate (the inverse of the lifetime), B is the radiative recombination rate,¹⁸ C_a is the ambipolar Auger coefficient,³ and G is a free carrier generation rate per unit volume. Surface recombination also has been introduced. The laser beam was assumed to have a Gaussian profile on the surface, absorbing exponentially with sample depth and expanding according to the Gaussian optics rules.

At the second step the equation for temperature distribution is solved,

$$-\nabla(k \nabla T) = Q. \quad (3)$$

Here k is the temperature dependent thermal conductivity,² and Q is the heat source term that is composed of two parts. The first part is the free carrier thermalization energy that is released at the point where the photon is absorbed, and the second part is a heating from bulk recombination and surface recombination obtained from the previous step.

It is possible to return to step 1, using temperature dependent parameters, then return to step 2 and continue until the iterations converge. Unfortunately we do not find experimental data on the temperature dependence of D_a for the concentration range of 10^{18} – 10^{19} cm⁻³, and C_a for $T > 400$ K. Another problem is the concentration dependence of the Au-

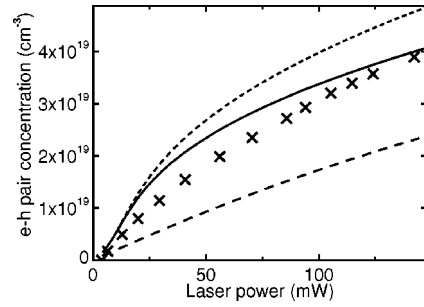


FIG. 12. Comparison between the experiment and numerical simulation results for the laser induced carrier concentration for 600 nm laser excitation: experimental points (crosses, same as at Fig. 7), simulation with the diffusion concentration dependence and Auger coefficient 1.1×10^{-30} cm⁶/s (solid line), Auger coefficient 3.8×10^{-31} cm⁶/s (short dashed), and simulation neglecting diffusion concentration dependence (long dashed).

ger coefficient³ C_a , which has been neglected in our model. At room temperature it changes from 3.8×10^{-31} cm⁶/s for high concentrations to 1.1×10^{-30} cm⁶/s for low concentration. At all concentration C_a increases with temperature.

Figure 12 compares the measured and the calculated free carrier concentrations for the 600 nm laser excitation (averaged for the Raman probing region). One has to take into account the temperature of the Si-SiO₂ interface which is high under the laser spot and may increase the value of C_a . The calculation has been performed for two values of the Auger coefficient C_a : 1.1×10^{-30} cm⁶/s (deliberately overestimated) and 3.8×10^{-31} cm⁶/s (slightly underestimated). One can see that in both cases the carrier concentration is overestimated in numerical simulation. In the concentration range of about 10^{19} cm⁻³ the room temperature value of D_a is about 1/3 of the low concentration value, due to carrier-carrier scattering. For the concentration range of about 10^{17} cm⁻³ the increase of D_a with temperature in the 300–420 K range has been observed experimentally.¹⁹ As a result of this numerical simulation we may assume that the temperature dependence of D_a for the 10^{19} cm⁻³ range is similar to the temperature dependence for the 10^{17} cm⁻³ range. The long dashed line in Fig. 12 presents the carrier concen-

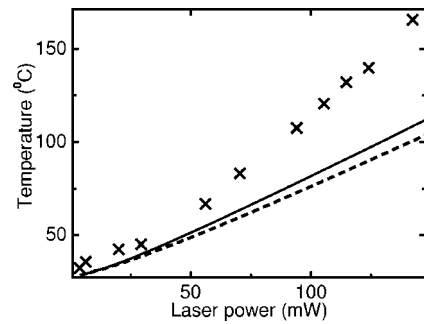


FIG. 13. Comparison between experiment and numerical simulation results for laser induced sample heating for the 600 nm laser wavelength: experimental points (crosses, same as in Fig. 5), simulation with the diffusion concentration dependence and Auger coefficient 1.1×10^{-30} cm⁶/s (solid line), and Auger coefficient 3.8×10^{-31} cm⁶/s (short dashed).

tration calculated with low concentration value of D_a , neglecting the carrier–carrier scattering. One can see that this approximation significantly underestimates the concentration, and the proper effective value for the diffusion coefficient lies between these two extremal cases.

Figure 13 presents a result of the second step of the numerical simulation—the average temperature. The slight underestimation of the temperature is attributed to an enhanced surface recombination under the laser spot, and possibly also to the flux dependent thermal conductivity.

V. CONCLUSION

In conclusion, we have presented the measurement of the asymmetric Fano-type line shape of the Raman spectrum of Si at high laser excitation densities. This line shape is attributed to the interference between phonon and photoexcited

holes Raman scattering processes. We demonstrated a new method for a precise determination of electron-hole plasma density from Raman measurements. It may be easily applied to a “pump-probe” measurement configuration. Spatial resolution of this method is limited by the wavelength in visible range, and is at least at factor 2 better than the resolution obtained by any method based on infrared measurements, such as photoluminescence or infrared absorption. It may be used for any Si sample, from intrinsic to heavily doped or damaged. This method may be used simultaneously with existing methods of electron-hole plasma characterization.

ACKNOWLEDGMENTS

This work has been made possible by a grant from the Israeli Ministry of Science and Arts.

*Electronic address: valya@ssrc.technion.ac.il

¹A. Compaan, M. Lee, and G. Trott, Phys. Rev. B **32**, 6731 (1985).

²*Properties of Silicon* (INSPEC, The Institution of Electrical Engineers, London and New York, 1988).

³P. Jonson, H. Bleichner, M. Isberg, and E. Nordlander, J. Appl. Phys. **81**, 2256 (1997).

⁴P. Altermatt, J. Schmidt, G. Heiser, and G. Aberle, J. Appl. Phys. **82**, 4938 (1997).

⁵C. Li, T. Sjödin, and H. Dai, Phys. Rev. B **56**, 15 252 (1997).

⁶V.I. Belitsky, A. Cantarero, M. Cardona, G. Trallero-Giner, and S. Pavlov, J. Phys.: Condens. Matter **9**, 5965 (1997).

⁷K. Arya, M. Kanehisa, M. Jouanne, K. Jain, and M. Balkanski, J. Phys. C **12**, 3843 (1979).

⁸M. Chandrasekhar, J. Renucci, and M. Cardona, Phys. Rev. B **17**, 1623 (1978).

⁹M. Jouanne, R. Beserman, I. Ipatova, and A. Subashiev, Solid State Commun. **16**, 1047 (1975).

¹⁰F. Cerdeira, T. Fjeldly, and M. Cardona, Phys. Rev. B **8**, 4734 (1973).

¹¹M. Balkanski, K. Jain, R. Beserman, and M. Jouanne, Phys. Rev. B **12**, 4328 (1975).

¹²N. Nickel, P. Lengsfeld, and I. Sieber, Phys. Rev. B **61**, 15 558 (2000).

¹³U. Fano, Phys. Rev. **124**, 1866 (1961).

¹⁴M. Wang and G. Xu, Appl. Opt. **38**, 2171 (1999).

¹⁵H. Burke and I. Herman, Phys. Rev. B **48**, 15 016 (1993).

¹⁶V. Fistul, *Heavily Doped Semiconductors* (Plenum, New York, 1969).

¹⁷J. Wagner, Phys. Rev. B **32**, 1323 (1985).

¹⁸H. Schlangenotto, H. Maeder, and W. Gerlach, Phys. Status Solidi B **21**, 357 (1974).

¹⁹M. Rosling, H. Bleichner, P. Jonsson, and E. Nordlander, J. Appl. Phys. **76**, 2855 (1994).